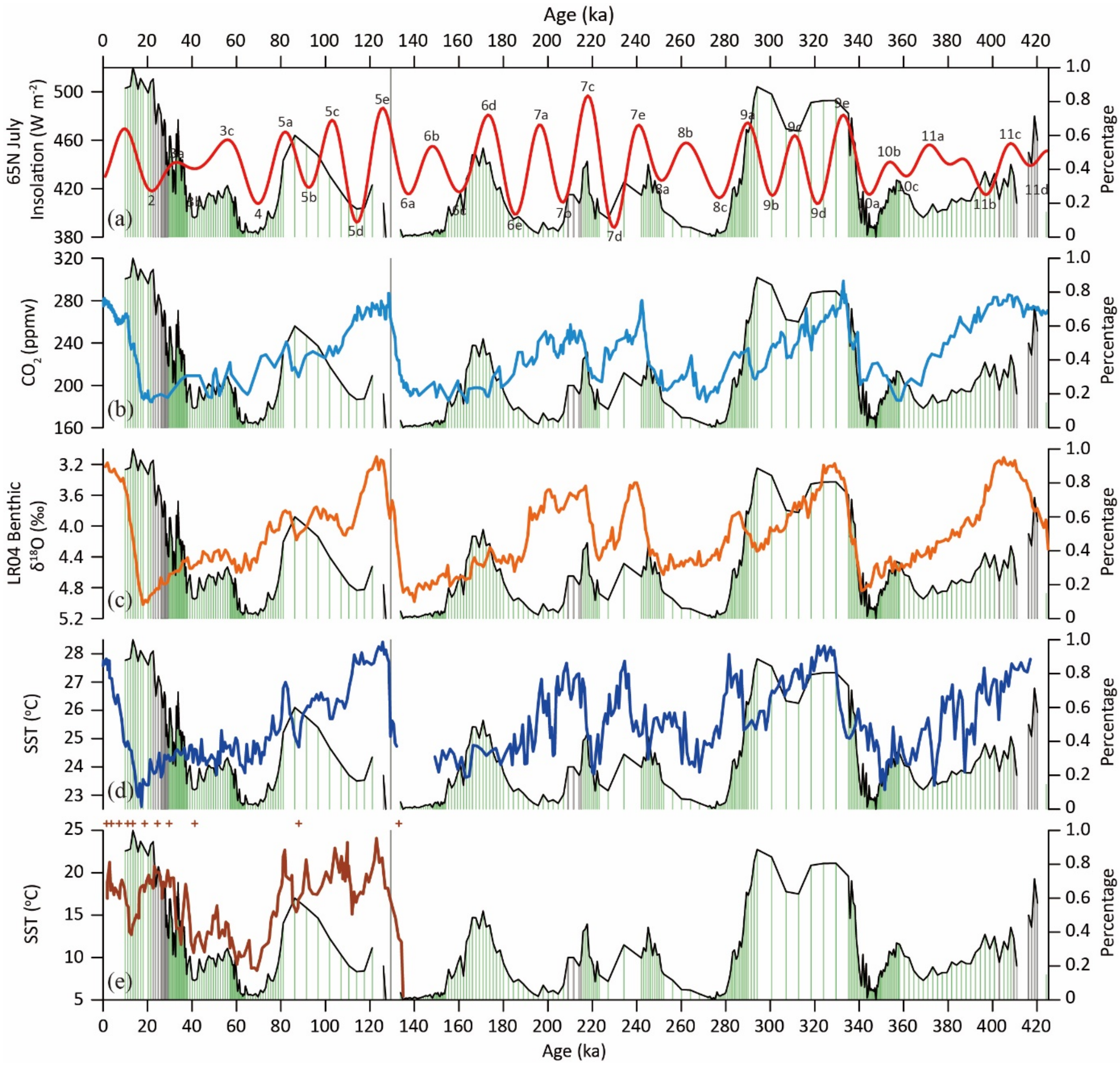

Supplementary Fig. 1. Snail fossil record from Luochuan, Chinese Loess Plateau. The percentage of warm snail species (Rousseau et al., 2009) compares to (a) the July insolation at 65 ^{o}N (red line, Berger and Loutre, 1991), (b) the atmospheric CO_2 levels (light blue line, Luthi et al., 2008), (c) the LR04 global benthic δ^{18}O stack (orange line, Lisiecki and Raymo, 2005), (d) the MD05-2901 alkenone SST from the South China Sea (dark blue line, Li et al., 2009) (e) the MD01-2408 alkenone SST from the Japan Sea (reddish brown line, Fujine et al., 2006). The percentage of warm snail species, an indicator for local climate, is anomalous high in glacial loess sediments during some periods, for example at ~360 ka, ~170 ka, and since ~40 ka. These warm events cannot be simply attributed to the increased NH summer insolation. In particular, in the last glacial-interglacial cycle, the regional warm trend starts since ~40 ka, while summer insolation, atmospheric greenhouse gas levels and tropical SST keep decreasing and NH ice volume keeps increasing until ~22 ka.

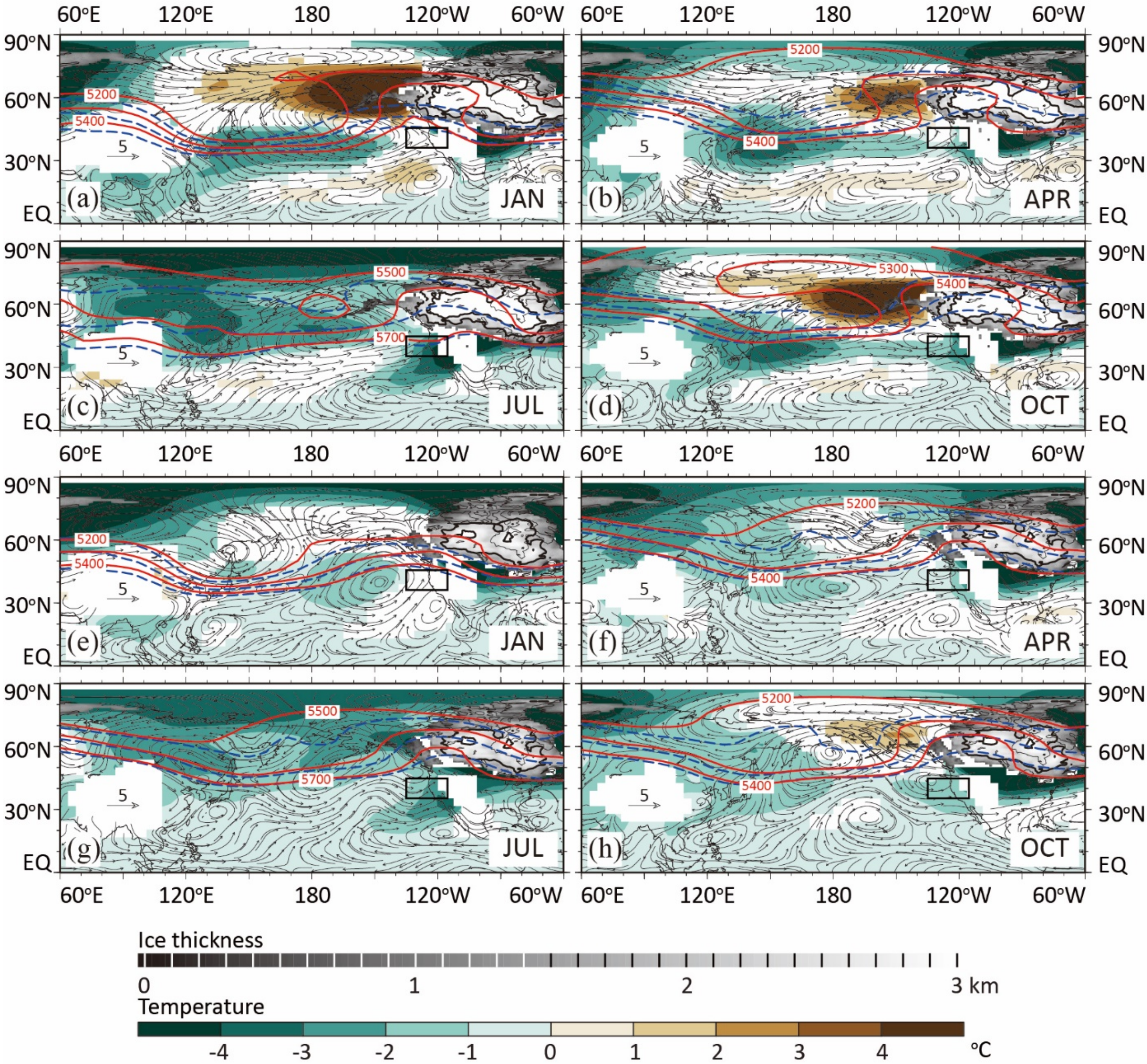

Supplementary Fig. 2. Climate sensitivity due to ICE6G Laurentide-Eurasian ice sheets. Upper four panels, changes in the 850 hPa winds (black arrows) and temperature (blue-brown shaded) due to the ICE6G ice sheet of 22 ka, (a) for Jan, (b) for Apr, (c) for Jul, and (d) for Oct. The grey shaded areas show the distribution and height of ice sheets. The black rectangle (between 35 and 45 ^{o}N, 115 and 135 ^{o}W) highlights the mid-latitude North American west coast, where DH, ODP Sites 1020 and 1014 are located. The three red lines show the simulated 500 hPa geopotential heights in the ice sheet sensitivity experiments, while the three dashed blue lines show the results in the reference experiments. Lower four panels, changes due to the ICE6G ice sheet of 70 ka, (e) for Jan, (f) for Apr, (g) for Jul, and (h) for Oct.

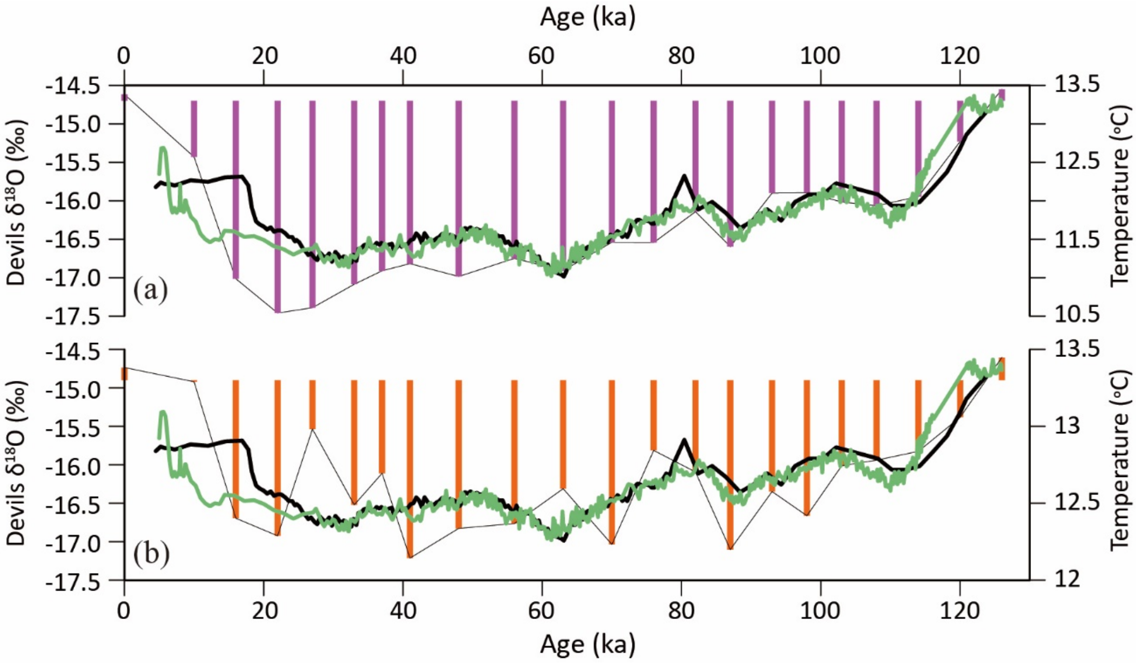

Supplementary Fig. 3. Simulated SAT evolution in mid-latitude North American west coast during last glacial-interglacial cycle. (a) The DH $\delta^{18}O$ (black line for DH-11 and green line for DH2-D, Landwehr et al., 2011; Moseley et al., 2016) and the SAT (light magenta bars) averaged over the mid-latitude North American west coast (the black rectangle shown in Supplementary Fig. 3) in the NorESM-ICE6G experiments, in which only the Laurentide-Eurasian ice sheets are included. As a comparison, (b) the DH $\delta^{18}O$ and the simulated regional SAT (orange bars) in the NorESM-BIOME4-PISM experiments with the Beringian ice sheet involved.

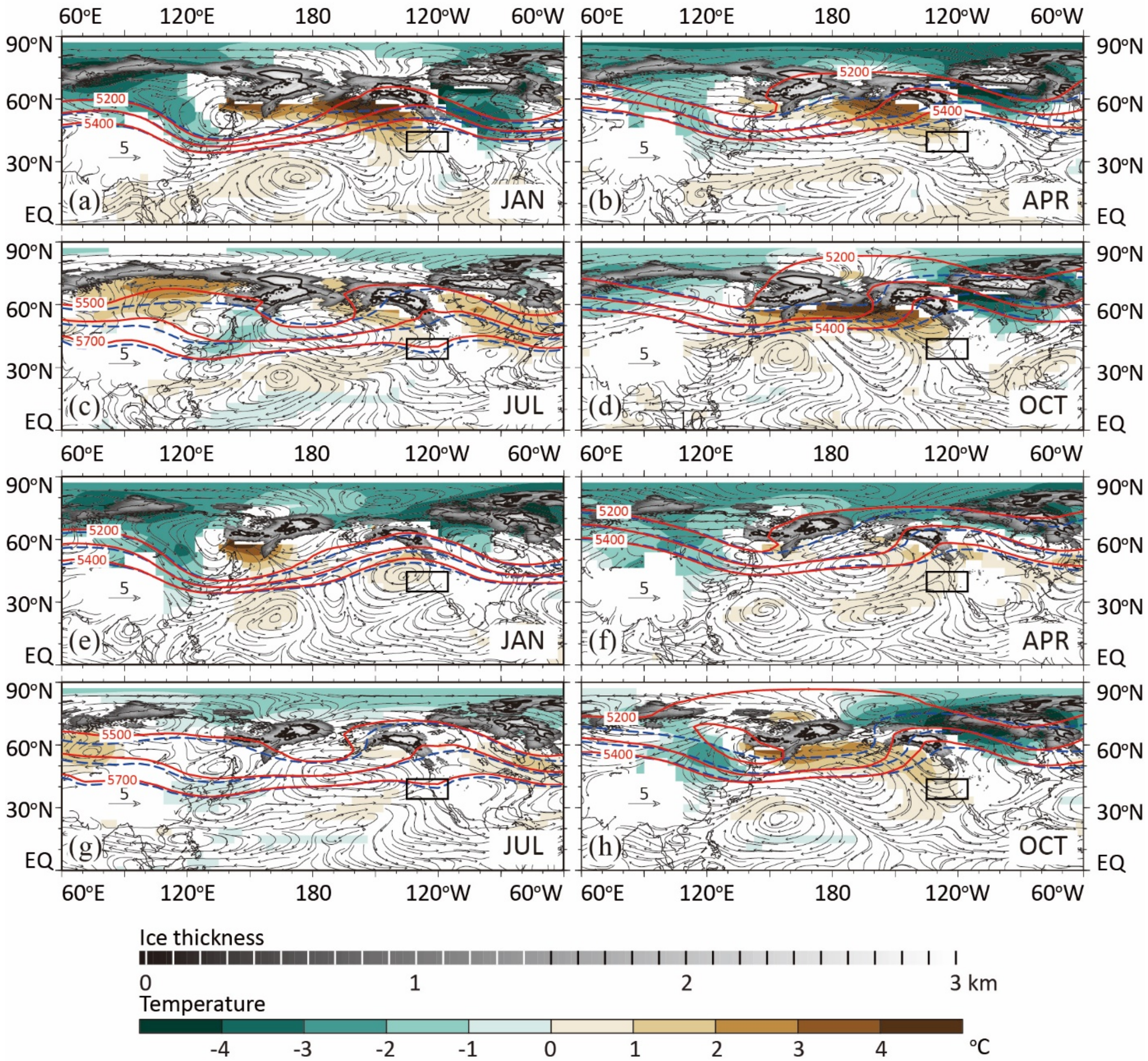

Supplementary Fig. 4. Climate sensitivity due to Beringian ice sheet. Upper four panels, changes in the 850 hPa winds (black arrows) and temperature (blue-brown shaded) due to the simulated Beringian ice sheet of 190 ka, (a) for Jan, (b) for Apr, (c) for Jul, and (d) for Oct. The grey shaded areas show the extent of ice sheets. The black rectangle (between 35 and 45 ^{o}N, 115 and 135 ^{o}W) highlights the mid-latitude North American west coast, where DH, ODP Sites 1020 and 1014 are located. The three red lines show the simulated 500 hPa geopotential heights in the ice sheet sensitivity experiments, while the three dashed blue lines show the results in the reference experiments. Lower four panels, changes due to the Beringian ice sheet of 114 ka, (e) for Jan, (f) for Apr, (g) for Jul, and (h) for Oct. Note the changes in 850 hPa temperature in the lower panels are much smaller than the reconstructed changes ~3-4 ^{o}C (Fig. 2).

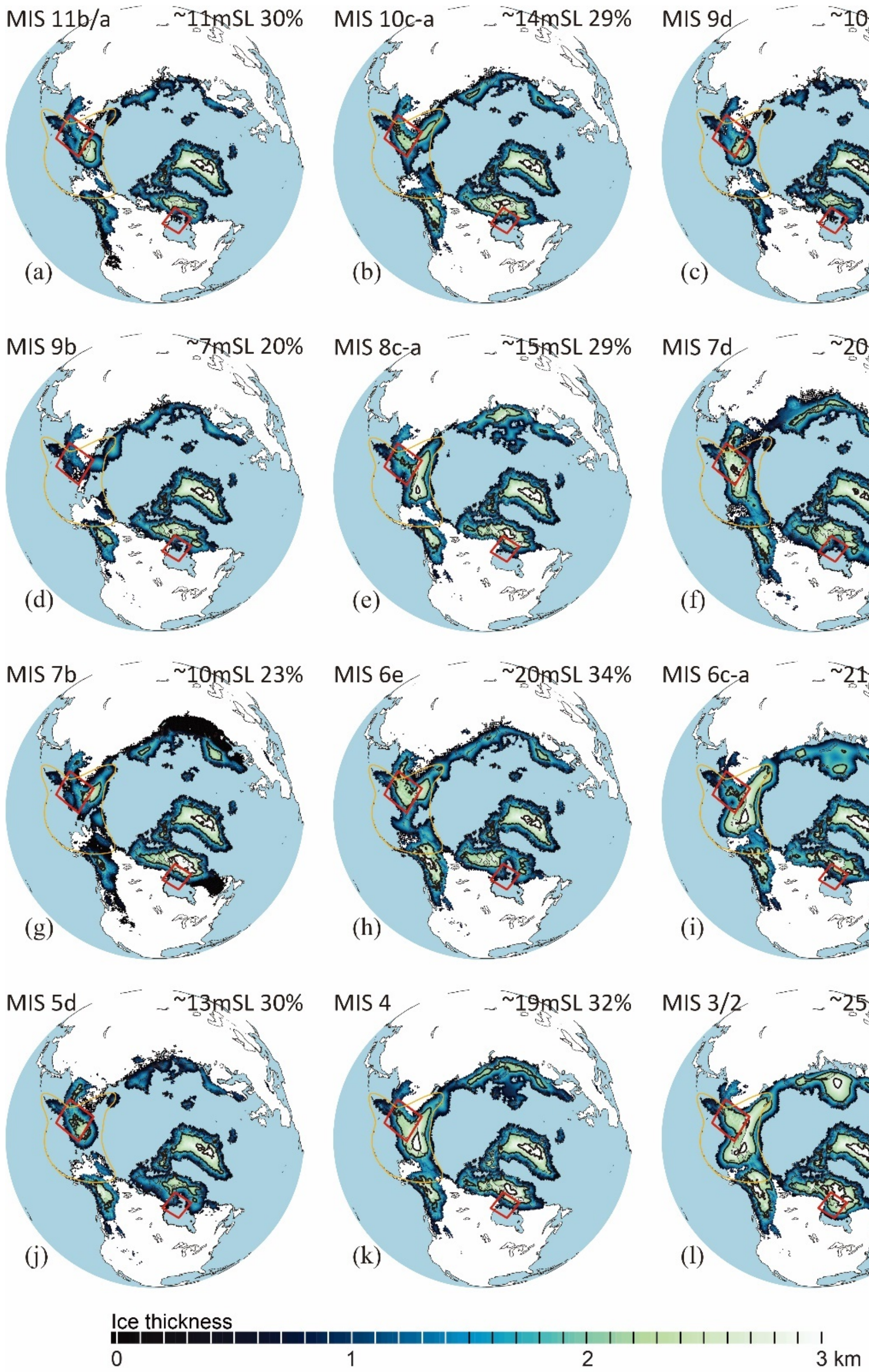

Supplementary Fig. 5. Simulated ice sheets during NE Siberian-Beringian glacials. We adopt the geographic definition of Beringia (Hoffecker, 2007), which includes the entire stretch from the Mackenzie River in Canada to the Lena River in NE Siberia. The yellow line outlines the area of Beringia. The two red boxes show the area of NE Siberia-Beringia and the North American east coast used in Supplementary Fig. 8. The ice volume of the Beringian ice sheet and it’s percentage in NH total ice volume are marked on the top-right corner of each panel.

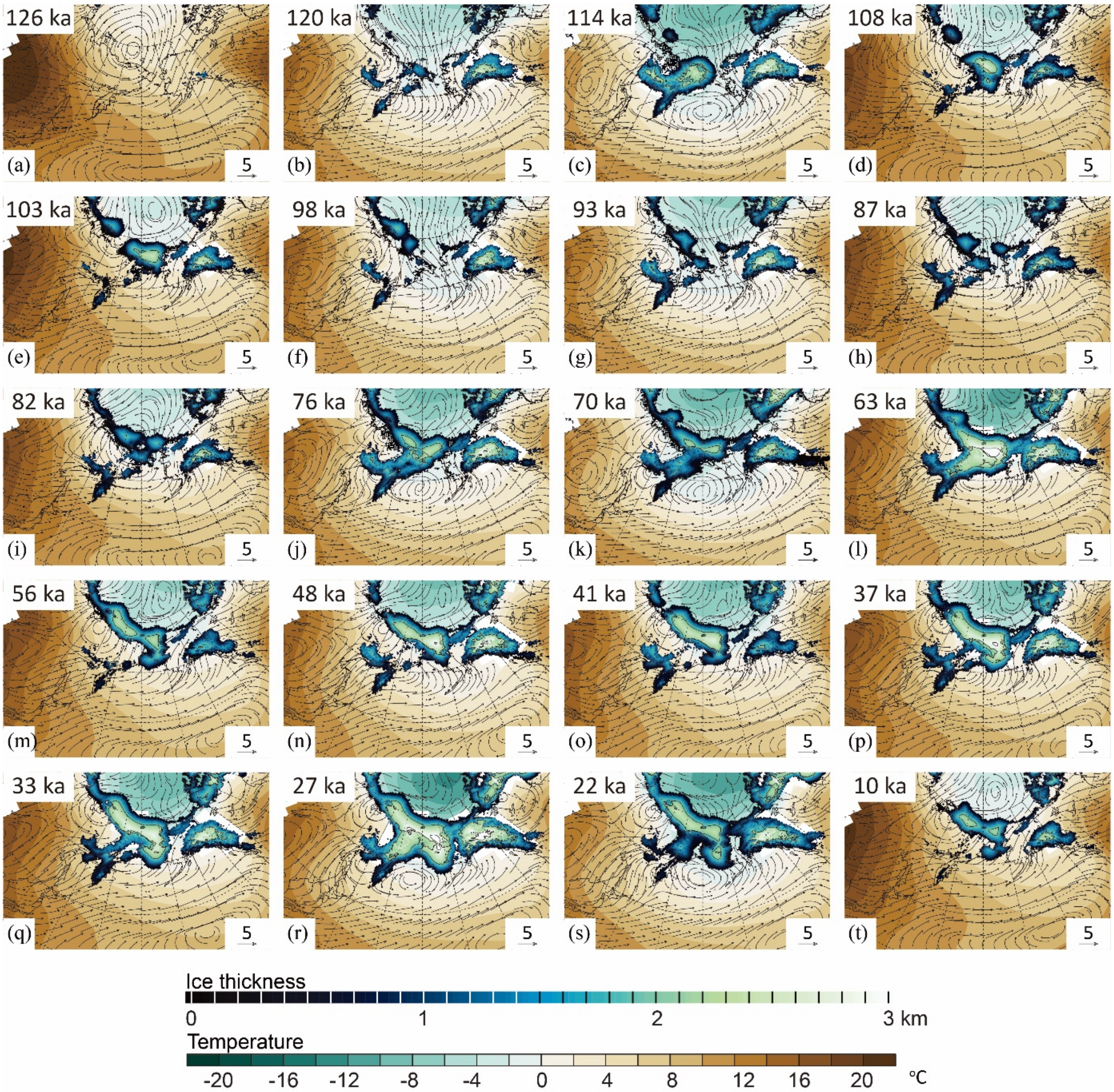

Supplementary Fig. 6. Simulated waxing and waning of Beringian ice sheet and summer climate during last glacial-interglacial cycle. Surface air temperature is shaded in blue and brown. 850hPa winds (m/s) are shown with arrows. Note the Beringian ice sheet exists during MIS5d (114 ka), MIS4 (j-l), and MIS3/2 (r). During the LGM, the NE Siberian-Beringian is largely gone (s), though a thin ice cover remains (see discussion for modelling uncertainties). Note the cyclonic wind anomalies over the Bering Sea. When the Beringian ice sheet does not exist or ice only exists on the NE Siberian continental shelf, almost no wind anomalies occur over the Bering Sea, for example MIS5c-a (d-i) and MIS3 (m-p).

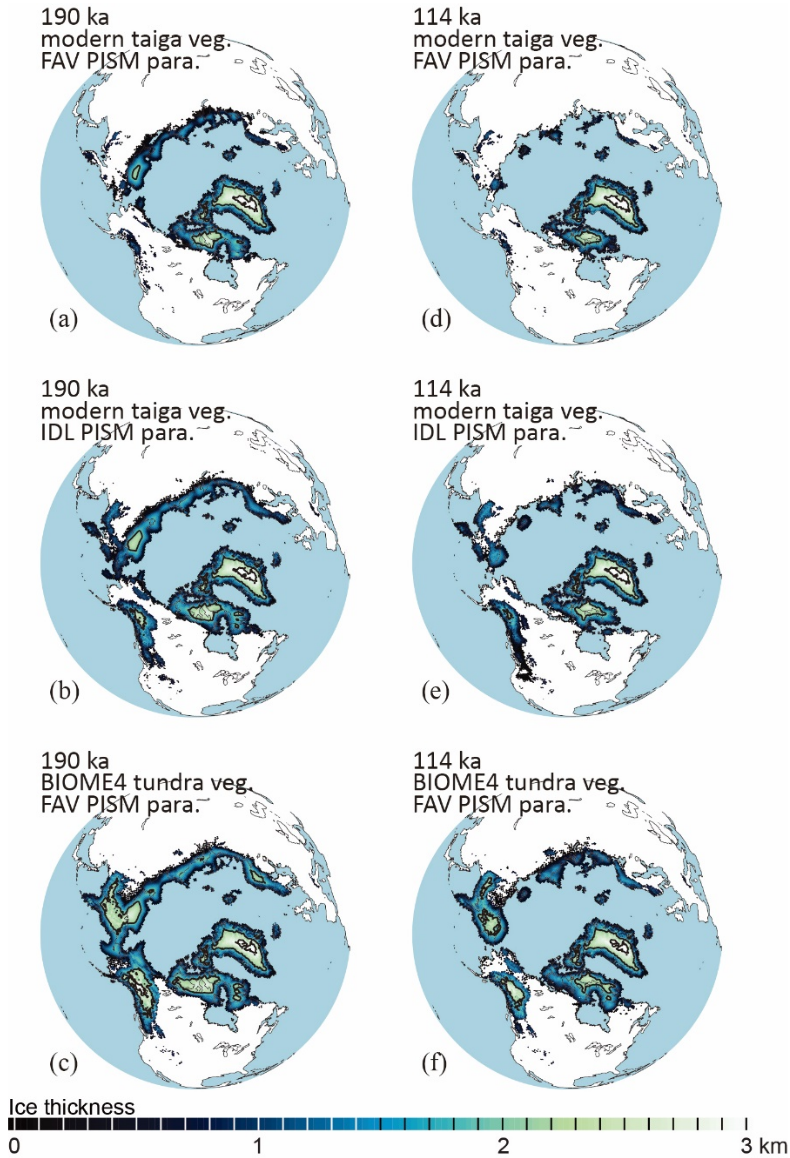

Supplementary Fig. 7. Vegetation feedbacks for inception of Beringian ice sheet. (a) and (d) the simulated ice sheets forced with the FAV PISM parameters and the climates simulated with modern vegetation conditions on NE Siberia-Beringia. (b) and (e) the simulated ice sheet forced with the IDL PISM parameters and the simulated climates with modern vegetation conditions on NE Siberia-Beringia. (c) and (f) the simulated ice sheet forced with the FAV PISM parameters, and the climates of 190 and 114 ka simulated with the BIOME4 glacial tundra vegetation conditions on NE Siberia-Beringia. These simulations demonstrate that a cooling due to the vegetation-albedo feedback is the key for the inception of the Beringian ice sheet.

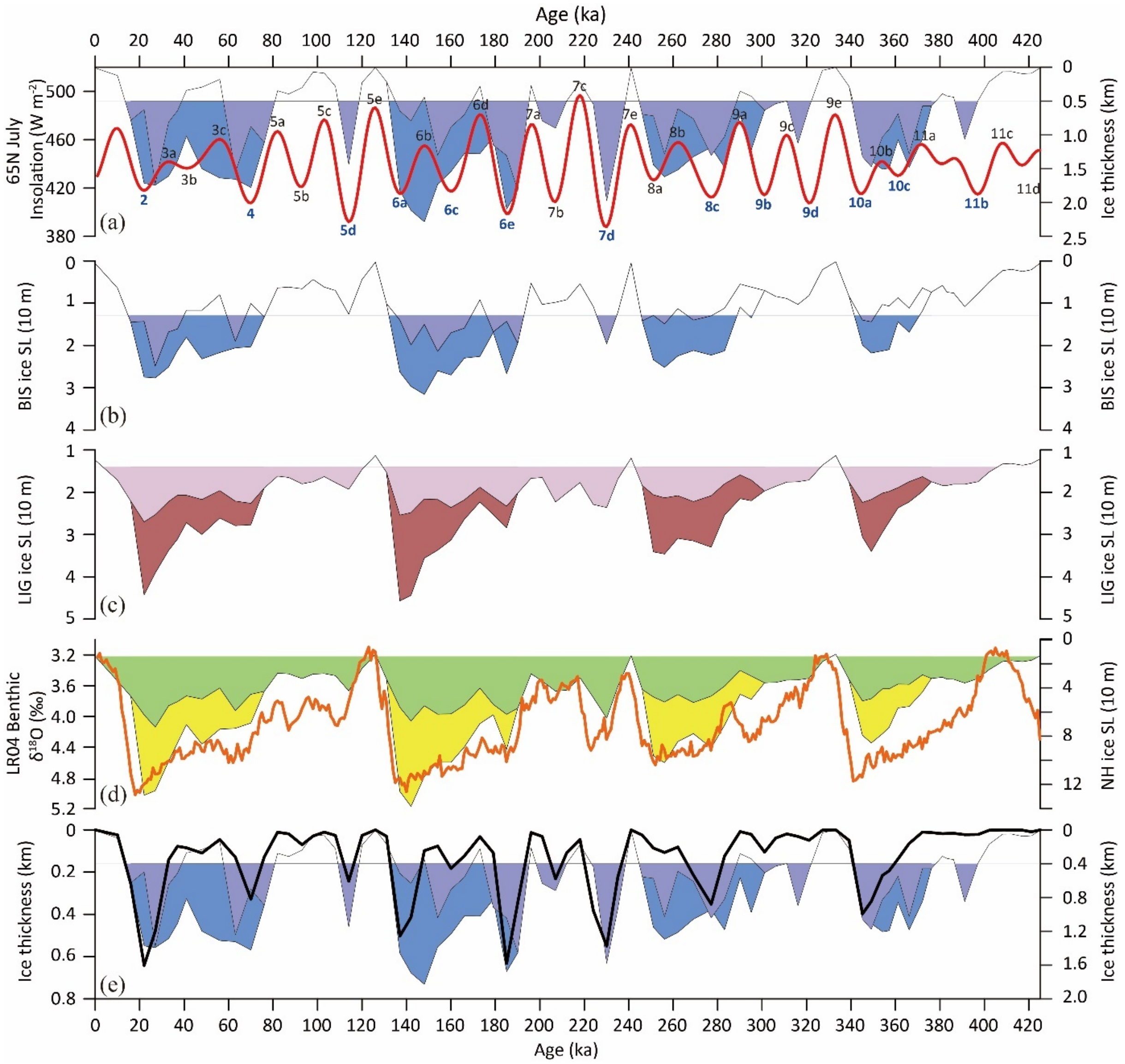

Supplementary Fig. 8. Comparison of simulated ice sheet with FAV and IDL PISM parameters. (a) The simulated ice height (purple shaded with the FAV parameters, light blue shaded with the IDL parameters) averaged over NE Siberia-Beringia (the red box in Supplementary Fig. 7) compared to the July insolation at 65°N (red line, Berger and Loutre, 1991). (b) The simulated ice volume for the Beringian ice sheet (equals to sea level equivalent, purple shaded with the FAV parameters, light blue shaded with the IDL parameters). (c) The simulated ice volume for the Laurentide-Innuitian-Greenland ice sheets (equals to sea level equivalent, light red shaded with the FAV parameters, dark red shaded with the IDL parameters). (d) The simulated total NH ice volume (equals to sea level equivalent, green shaded with the FAV parameters, yellow shaded with the IDL parameters) compared to the LR04 global benthic δ^{18}O stack (orange line, Lisiecki and Raymo, 2005). (e) The simulated ice height with the FAV parameters averaged over NE Siberia-Beringia (purple shaded) and the North American east coast (bold black line).